In the 500 ml Ravussin groups it is notable that even the lowest ventilatory frequency (4 bpm with I:E ratio of 1:2) was associated with elevated end-inspiratory lung pressures and reduced DO_2 and cardiac output. This would suggest that a ventilatory frequency of 4 bpm with an expiratory time of 10 s may still produce dynamic hyperinflation. The RPH jetting strategy recognises this: subsequent jets are not delivered until peripheral oxygen saturation has peaked and then started to decline. The time between jets is thus often minutes rather than seconds.

Re-oxygenation was achieved rapidly and maintained, even with very small tidal volumes and low ventilatory frequencies, highlighting that when the upper airway is obstructed very little oxygen needs to be delivered in order to re-oxygenate a patient. This has been observed experimentally in large animal models[6] and is in keeping with our ovine model, where a saturation response after a single jet is typically seen at a median of 13 s and maintained despite jetting subsequently at a rate of less than once per minute.[7]

In this simulation study, the Pa_{co2} was 11.1 kPa at the end of apnoea and increased to more than 15 kPa by the end of the 5-min rescue period when very small tidal volumes were delivered. These simulated patients did not appear to manifest cardiovascular compromise related to hypercarbia. This would appear to support the premise of the RPH CICO management strategy in which very low minute volume oxygen delivery via a cannula is a temporising measure. Part of the strategy is that a cuffed airway is inserted within a matter of minutes, once critical hypoxaemia has been averted.

Laviola and colleagues[1] provide evidence that we must deliver 'only enough oxygen as required to oxygenate' if we are to safely use narrow-bore cannula cricothyroidotomy. When using cannula techniques, we must now refrain from ventilating for a few minutes and be satisfied by treating life-threatening hypoxaemia.

Declarations of interest

All have taught, presented, or published on CICO rescue techniques. Many of the CICO courses have received training equipment from Cook, VBM, and Meditech. AH has received funds from sales of his eBook, which have been used to support CICO courses.

References

1. Laviola M, Niklas C, Das A, Bates DG, Hardman JG. Effect of oxygen fraction on airway rescue: a computational modelling study. *Br J Anaesth* 2020; **125**: e69–74
2. Heard A. *Percutaneous emergency oxygenation strategies in the 'Can't Intubate, Can't Oxygenate' scenario*. Smashworks Editions; 2013. Available from: https://www.smashwords.com/books/view/377530. [Accessed 28 April 2021]
3. All Wales Airway Group Approach to CICO https://allwalesairwaygroup.co.uk/file/view/122 (accessed 2 June 2021)
4. Schechtman SA, Buist M, Cloyd BH, Tremper KK, Healy DW. The OxyTain algorithm: an adaptation of existing emergency front of neck access approaches within a North American tertiary referral health care system. *A A Pract* 2019; **13**: 405–6
5. Holmdahl M. Pulmonary uptake of oxygen, acid-base metabolism and circulation during prolonged apnoea. *Acta Chir Scand* 1956; **S212**: 1–128
6. Black IH, Janus SA, Grathwohl KW. Low-flow transtracheal rescue insufflation of oxygen after profound desaturation. *J Trauma* 2005; **59**: 344–9
7. Mayer J, Heard AMB, Dinsmore JE. Initial data from single jet rescue oxygenation in critical hypoxia. *Anaesthesia* 2011; **66**: 232–8

doi: 10.1016/j.bja.2021.05.010
Advance Access Publication Date: 10 June 2021

Quantification of lobar gas exchange: a proof-of-concept study in pigs

Jack Gallifant[1], John N. Cronin[1,2,**] and Federico Formenti[1,3,4,*]

[1]Centre for Human and Applied Physiological Sciences, School of Basic and Medical Biosciences, King's College London, London, UK, [2]Department of Anaesthesia, Guy's and St Thomas' NHS Foundation Trust, London, UK, [3]Nuffield Division of Anaesthetics, University of Oxford, Oxford, UK and [4]Department of Biomechanics, University of Nebraska Omaha, Omaha, NE, USA

*Corresponding author.

**Corresponding author. E-mails: john.n.cronin@kcl.ac.uk, federico.formenti@outlook.com

Keywords: bronchoscopy; lung; lung function tests; oxygen consumption; pulmonary gas exchange

Editor—The prediction of postoperative lung function helps to stratify lung cancer patients' risk of mortality and potential suitability for resection.[1] Carbon monoxide transfer (T_{LCO}) and forced expiratory volume in 1 s (FEV_1) tests are commonly used to determine diffusion capacity and degree of airway obstruction respectively, and to predict post-resection dyspnoea, assuming they would decrease in proportion to the number of lung segments resected. These tests provide global indicators of lung function, but cannot distinguish between functional contributions from different lobes.

Gas exchange occurs heterogeneously, differing between lung regions in health and disease,[2] and this heterogeneity can be exaggerated by lung cancer, limiting the usefulness of whole-lung function tests. Estimates of postoperative FEV_1 based upon CT measurements of resected lung volume[3] or quantitative ventilation/perfusion scintigraphy[1] may be more informative. However, these methods are limited by poor correlation between postoperative FEV_1 and functional capacity, where maximal oxygen uptake is more sensitive.[4] Quantifying lobar contribution to overall pulmonary gas exchange could provide more accurate predictions of postoperative lung function. For example, if a diseased lobe contributes minimally to gas exchange, its resection will be unlikely to have a major functional impact.

The aim of this study was to measure oxygen uptake at the lobar level in a proof-of-concept experimental study. A fibreoptic sensor was used to measure tidal variation in lobar partial pressure of oxygen (P_{O_2}), and whole-lung CT to quantify lobar tidal volume; these measurements combined were used to calculate lobar oxygen uptake. This study, conducted in the Hedenstierna Laboratoriet at Uppsala University, Sweden, received ethical approval (AREC ref.C98/16) and conformed with the National Institutes of Health (NIH) and Animal Research: Reporting of *In Vivo* Experiments (ARRIVE) guidelines.[5]

Two male domestic pigs (29 kg) were studied in dorsal recumbency under general anaesthesia and mechanical ventilation via tracheostomy; details of the anaesthesia protocol are presented elsewhere.[6] Mechanical ventilation was delivered by a Servo-I ventilator (Maquet, Rastatt, Germany) in pressure-control mode with tidal volume of 10 ml kg^{-1}, ventilatory frequency of 12 breaths min^{-1}, inspiratory/expiratory (I/E) ratio of 1:2, and inspiratory rise time of 0 s so each breath consisted of 1.67 s of inspiration and 3.33 s of expiration. A saline lavage surfactant-depletion lung-injury model was induced in one pig to study heterogeneous lungs.[6]

Cardiopulmonary variables (IntelliVue M8004A, Philips Healthcare, Amsterdam, the Netherlands; Capnomac Ultima, Datex-Ohmeda, Madison, WI, USA) and lobar P_{O_2} (OxyLite Pro, Oxford Optronix, Abingdon, UK) were continuously monitored, with analogue signals digitised using PowerLab (ADInstruments, Dunedin, New Zealand) and recorded with LabChart version 8.2.1 (ADInstruments) at a sampling rate of 10 Hz throughout. Data were processed using R version 3.6.2 (R Foundation for Statistical Computing, Vienna, Austria; www.r-project.org).

P_{O_2} was recorded with fibreoptic sensors with a response time of <150 ms in air.[7] The sensor working principle is based on luminescence quenching by oxygen of a fluorophore embedded in a polymer material with technical details as described elsewhere.[7–10] The fine-bore sensor was inserted into a bronchoscope until the sensor tip was visible inside the main bronchus entering a lobe, with the bronchoscope itself remaining within the large airways. Data for ~12 breaths were collected in each lobe and averaged to produce a single breath per lobe. P_{O_2} tidal variation was calculated as the peak-to-trough difference in the averaged breath. Tidal variation in lobar P_{O_2} (kPa) was then converted to tidal variation in oxygen concentration (DeltaP_{O_2}, %), dividing by 101.3 kPa. This experiment could not be completed in the CT scanner, so lobar P_{O_2} measurements were completed just before CT imaging.

Whole-lung volume CT scans (Somatom Definition Flash; Siemens Healthcare, Forchheim, Germany) were recorded during end-inspiratory and end-expiratory breath-holding manoeuvres (under the same ventilation conditions as during the lobar P_{O_2} experiment) to measure lobar tidal volume. Lobar volumes were calculated via segmentation at 3-mm intervals using 3D Slicer version 4.1 (https://www.slicer.org); Figure 1a–c illustrates the segmentation process. Gas volumes were then calculated as

$$\text{Lobar gas volume (ml)} = \text{Lobar volume}\left(\text{cm}^3\right) \times \frac{-[\text{Mean voxel density (HU)}]}{1000},$$

and lobar oxygen uptake was calculated by multiplying tidal gas volume (difference between end-inspiratory and end-expiratory lobar gas volumes) by DeltaP_{O_2} (%). Further methodological details are presented in Supplementary Table S1, which shows the baseline characteristics of the animals studied. Cardiorespiratory parameters were within the normal or expected range, with a lower P/F ratio in the lung injury model (15.1 kPa) than in the control (61.5 kPa). In order to achieve normoxaemia, inspired oxygen concentration was higher in the lung injury model (0.7 *vs* 0.4 [control]).

Figure 1d illustrates the lobar P_{O_2} tidal variation, greater in the saline lavage lung injury model than in the control pig. Figure 1 inset table presents lobar P_{O_2}, end-inspiratory, end-expiratory and tidal volumes, and the associated lobar oxygen uptake. P_{O_2} tidal variation ranged from 4.7 to 20.3 kPa in different lobes. Lobar tidal volume ranged from 12.9 to 75.1 ml, with lobar oxygen uptake ranging from 0.6 to 11.9 ml $breath^{-1}$. Figure 1e shows oxygen uptake in both animals, visualising the difference between lobes, and overall pulmonary oxygen uptake between animals.

These results demonstrate the feasibility of a novel technique to calculate lobar oxygen uptake in a mechanically ventilated control and saline lavage lung injury pig model. Study limitations include the small sample size and use of a porcine model that do not fully replicate all features of the human respiratory system. Data were collected at rest, assuming proportional contributions during exercise, when functional limitation likely occurs. Nevertheless, the lung injury model used resulted in heterogeneous lung injury and hypoxaemia, and was sufficient to determine differences in lobar and overall oxygen uptake compared with the control.

The distribution of lobar contribution to gas exchange can vary significantly, even in patients with similar overall lung function, but tests currently used to predict lung function after lung cancer resection cannot determine gas exchange at the lobar level. After refinement, the technique proposed here could provide valuable insight into the proportion of oxygen uptake associated with a given lobe and support the decision on patients' suitability for lobar resection. Although this technique was tested under conditions of general anaesthesia and mandatory ventilation, its working principle would remain valid during spontaneous breathing, allowing use of the technique in the outpatient setting. The technique is

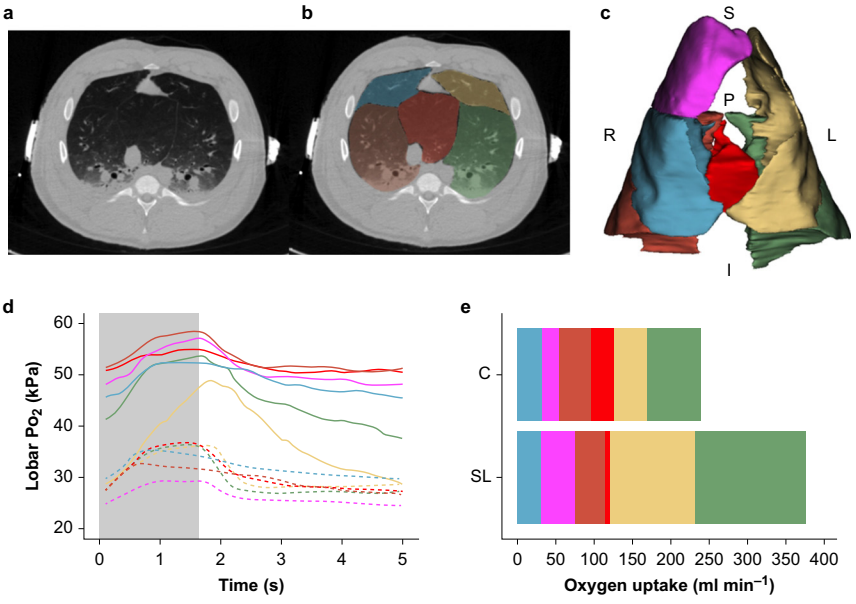

Lobe	Animal	Po_2 Mean	Po_2 Max	Po_2 Min	Po_2 Delta	Po_2 Delta	Density Mean	Volume End-Inspiratory	Volume End-Expiratory	Volume Tidal	Oxygen uptake per breath	Oxygen uptake Proportion of total lung
		kPa				%	HU	mL			mL breath^{-1}	%
Left Caudal	SL	45.6	53.6	37.5	16.1	**16**	–247.5	105.2	30.1	**75.1**	11.9	**38**
	C	29.8	36.4	26.8	9.6	**9**	–367.4	112.3	51.3	**61.0**	5.8	**29**
Left Cranial	SL	37.3	48.9	28.6	20.3	**20**	–450.1	97.1	50.6	**46.5**	9.3	**30**
	C	30.7	36.2	27.9	8.3	**8**	–548.3	95.9	52.0	**43.9**	3.6	**18**
Right Accessory	SL	52.0	55.0	50.3	4.7	**5**	–334.8	23.8	10.9	**12.9**	0.6	**2**
	C	30.8	36.7	27.2	9.4	**9**	–571.2	43.8	17.7	**26.1**	2.4	**12**
Right Caudal	SL	53.3	58.1	50.6	7.6	**8**	–153.6	59.5	15.3	**44.3**	3.3	**11**
	C	29.6	32.9	26.6	6.3	**6**	–341.4	104.2	46.6	**57.6**	3.6	**18**
Right Cranial	SL	51.1	57.0	47.9	9.1	**9**	–451.4	86.4	45.1	**41.3**	3.7	**12**
	C	26.4	29.4	24.4	5.0	**5**	–562.6	84.1	48.0	**36.1**	1.8	**9**
Right Middle	SL	48.9	52.5	45.4	7.1	**7**	–472.6	75.9	40.1	**35.8**	2.5	**8**
	C	31.9	35.4	29.5	5.9	**6**	–672.3	115.3	69.8	**45.5**	2.7	**13**

Fig 1. Computed tomography scans and associated three-dimensional reconstruction of the porcine lung, lobar partial pressure of oxygen (lobar Po_2) measured during a respiratory cycle, and lobar and whole lung oxygen uptake. Same axial slice from the same pig: (a) the original image; (b) the lobes labelled by colour (left caudal, green; left cranial, yellow; right accessory, red; right caudal, orange; right cranial, pink; right middle, blue). This colour coding is also used in panels c, d, and e. (c) A three-dimensional reconstruction of the control pig lungs at end-inspiration, viewed from anterior to posterior. I, inferior; S, superior; R, right; L, left. (d) Lobar partial pressure of oxygen (Po_2) recorded with fibreoptic technology at 0.1-s intervals during a respiratory cycle for each lobe (data averaged over at least three cycles); dashed and solid lines show values for the control and saline lavage lung injury pig, respectively. The shaded (left) and clear (right) regions in (d) indicate inspiration and expiration, respectively. Recordings were made during pressure-controlled mechanical ventilation, with tidal volume 10 ml kg^{-1}, I/E ratio 1:2, and ventilatory frequency 12 breaths min^{-1}. (e) Lobar and whole lung oxygen uptake (ml min^{-1}). Inset table: lobar densities and volumes were calculated from CT images recorded during end-inspiratory and end-expiratory breath-holding manoeuvres. Lung segmentation started at the bifurcation of the trachea. Rounding to the nearest % performed. Po_2, partial pressure of oxygen; HU, Hounsfield units; C, control pig; SL, saline lavage lung injury model.

clinically feasible given the widespread use of both bronchoscopy and CT imaging in lung cancer diagnosis.

Acknowledgements

We are grateful to Rongsheng Chen and Oxford Optronix for making the fibreoptic oxygen sensors available, to Dr Douglas Crockett, to Dr João Batista Borges and to the staff in the Hedenstierna Laboratoriet and in the Radiology Department, Uppsala University Hospital, including Agneta Roneus, Kerstin Ahlgren, Mariette Anderson, Liselotte Pihl, Maria Swälas, Monica Segelsjö, Göran Hedenstierna, Anders Larsson, and Miklos Lipcsey for their support with data collection.

Declarations of interest

The authors declare that they have no conflicts of interest.

Funding

Medical Research Council (MC_PC_17164). FF contributed to financial support.

Appendix A. Supplementary data

Supplementary data to this article can be found online at https://doi.org/10.1016/j.bja.2021.04.022.

References

1. Lim E, Baldwin D, Beckles M, et al. Guidelines on the radical management of patients with lung cancer. *Thorax* 2010; **65**. iii1–27
2. Wagner PD. The physiological basis of pulmonary gas exchange: implications for clinical interpretation of arterial blood gases. *Eur Respir J* 2015; **45**: 227–43
3. Papageorgiou CV, Antoniou D, Kaltsakas G, Koulouris NG. Role of quantitative CT in predicting postoperative FEV1 and chronic dyspnea in patients undergoing lung resection. *Multidiscip Respir Med* 2010; **5**: 188
4. Wang JS, Abboud RT, Wang L-M. Effect of lung resection on exercise capacity and on carbon monoxide diffusing capacity during exercise. *Chest* 2006; **129**: 863–72
5. Kilkenny C, Browne WJ, Cuthill IC, Emerson M, Altman DG. Improving bioscience research reporting: the ARRIVE guidelines for reporting animal research. *PLoS Biol* 2010; **8**, e1000412
6. Lachmann B, Robertson B, Vogel J. In vivo lung lavage as an experimental model of the respiratory distress syndrome. *Acta Anaesthesiol Scand* 1980; **24**: 231–6
7. Chen R, Formenti F, Obeid A, Hahn CE, Farmery AD. A fibre-optic oxygen sensor for monitoring human breathing. *Physiol Meas* 2013; **34**: N71–81
8. Formenti F, Bommakanti N, Chen R, et al. Respiratory oscillations in alveolar oxygen tension measured in arterial blood. *Sci Rep* 2017; **7**: 7499
9. Formenti F, Chen R, McPeak H, Matejovic M, Farmery AD, Hahn CE. A fibre optic oxygen sensor that detects rapid PO2 changes under simulated conditions of cyclical atelectasis in vitro. *Respir Physiol Neurobiol* 2014; **191**: 1–8
10. Crockett DC, Cronin JN, Bommakanti N, et al. Tidal changes in PaO_2 and their relationship to cyclical lung recruitment/derecruitment in a porcine lung injury model. *Br J Anaesth* 2019; **122**: 277–85

doi: 10.1016/j.bja.2021.04.022
Advance Access Publication Date: 9 June 2021

Location of the entry point of the muscular branch of the nerve to vastus medialis

Eman Nada[1,*], Amr Elmansoury[2,3], Nabil Elkassabany[4] and Elizabeth R. Whitney[2]

[1]Department of Anesthesiology and Perioperative Medicine, University of Massachusetts Medical School, Worcester, MA, USA, [2]Department of Anatomy and Neurobiology, Boston University School of Medicine, Boston, MA, USA, [3]Massachusetts College of Pharmacy and Health Sciences, Worcester, MA, USA and [4]Department of Anesthesiology and Critical Care, University of Pennsylvania, Philadelphia, PA, USA

*Corresponding author. E-mail: Eman.Nada@umassmemorial.org

Keywords: adductor canal block; cadaver; femoral triangle; nerve block; quadriceps weakness; vastus medialis

Editor—Blocking the nerve to vastus medialis can be the cause of occasional motor weakness identified after adductor canal block (ACB), a common procedure for pain control after knee and leg surgery. Although it results in less quadriceps muscle weakness compared with femoral nerve block, significant motor weakness is occasionally seen.[1,2] The quadriceps weakness observed after ACB may be related to the spread of the local anaesthetics proximally, to the femoral nerve, or as